Hematopoietic progenitor cell lines with myeloid and lymphoid potential

Vanessa Redecke[1], Ruiqiong Wu[1], Jingran Zhou[1], David Finkelstein[2], Vandana Chaturvedi[1], Anthony A High[3] & Hans Häcker[1]

Investigation of immune-cell differentiation and function is limited by shortcomings of suitable and scalable experimental systems. Here we show that retroviral delivery of an estrogen-regulated form of Hoxb8 into mouse bone marrow cells can be used along with Flt3 ligand to conditionally immortalize early hematopoietic progenitor cells (Hoxb8-FL cells). Hoxb8-FL cells have lost self-renewal capacity and potential to differentiate into megakaryocytes and erythrocytes but retain the potential to differentiate into myeloid and lymphoid cells. They differentiate *in vitro* and *in vivo* into macrophages, granulocytes, dendritic cells, B lymphocytes and T lymphocytes that are phenotypically and functionally indistinguishable from their primary counterparts. Quantitative *in vitro* assays indicate that myeloid and B-cell potential of Hoxb8-FL cells is comparable to that of primary lymphoid-primed multipotent progenitors, whereas T-cell potential is diminished. The simplicity of this system and the unlimited proliferative capacity of Hoxb8-FL cells will enable studies of immune-cell differentiation and function.

The conserved family of *Hox* genes encodes 39 transcription factors in mammals, which control many aspects of embryonic development and hematopoiesis[1]. In hematopoiesis, *Hox* genes are preferentially expressed in immature progenitor cells and hematopoietic stem cells[2]. A substantial body of evidence suggests that one important function of *Hox* genes is to increase cell self-renewal and to arrest cell differentiation[1]. This property has been previously used to establish stably growing, homogenous hematopoietic progenitor cell lines through retrovirus-mediated expression of certain *Hox* genes, such as *Hoxa9* and *Hoxb8* (ref. 3). These data also established that a specific growth factor, stem cell factor (SCF) versus granulocyte-macrophage colony-stimulating factor (GM-CSF), in the context of *Hox* gene expression, can be used to establish progenitor cell lines committed to different lineages, that is, the granulocyte (SCF) and monocyte (GM-CSF) lineage, respectively.

Given the critical role of Flt3 in generation of dendritic cells[4,5], we evaluated the possibility that Flt3 ligand (Flt3L) in combination with activated Hoxb8 could be used to immortalize dendritic cell progenitors. Starting from largely unfractionated bone marrow (BM) cell preparations, we observed that the combination of Hoxb8 and Flt3L could in fact lead to the generation of cells that not only differentiate into dendritic cells but that retain the potential to differentiate into both lymphoid and myeloid lineages. We describe the establishment of this cell culture system and characterize the resulting Hoxb8-FL cells, providing a powerful tool for the investigation of differentiation and function of immune cells.

## RESULTS

Generation of Hoxb8-FL cells

We infected BM cells, which we had briefly expanded *in vitro*, with a murine stem cell virus (MSCV)-based retrovirus expressing an estrogen-regulated form of Hoxb8, a fusion construct of Hoxb8 and the hormone-binding domain of the estrogen receptor, ERHBD (ERHBD-HoxB8; **Supplementary Fig. 1**), followed by cell culture in the presence of estrogen and Flt3L. In the absence of virus expressing ERHBD-Hoxb8, cells did not expand and differentiated into typical dendritic cells, as expected[5] (**Fig. 1a**). However, in the presence of estrogen-activated Hoxb8 and Flt3L, blast-like cells expanded with exponential growth characteristics (**Fig. 1**). Growth and survival of these cells strictly depended on the presence of Flt3L (**Fig. 1b,c**). We could stably culture Hoxb8-FL cells for many weeks and also could subclone them (see below). Flt3L can thus be used to generate Hoxb8-driven, growth factor–dependent cell lines.

Potential to differentiate into myeloid cells *in vitro*

We withdrew estrogen (to inactivate Hoxb8) and analyzed growth and phenotype of cells obtained in the presence of Flt3L. For comparison, we used primary BM cells. Upon withdrawal of estrogen, Hoxb8-FL cells continued to expand until around day 6 and stayed largely alive until day 8 (**Fig. 1b**). Phenotypic changes started to appear at about day 3, with a decrease in nucleus to cytoplasm ratio, slightly higher expression of CD11b and B220 on some cells, and downregulation of c-Kit, which was highly expressed

Figure 1 | Growth and morphology of Hoxb8-FL cells. (**a**) Cell numbers over time of BM cells infected with an MSCV-based retrovirus expressing ERHBD-Hoxb8 and cultured in estrogen and Flt3L. Error bars, s.d. ($n = 5$ wells). (**b**) Numbers of cells grown in medium with indicated factors, starting from 2×10^5 exponentially growing Hoxb8-FL cells. Mean cell numbers obtained after 8 d of culture were: Flt3L, 1.6×10^6; GM-CSF, 1.3×10^6; M-CSF, 4.5×10^6. Error bars, s.d. ($n = 3$ Hoxb8-FL cell populations). (**c–f**) Micrographs of Hoxb8-FL cells grown in medium without growth factor (**c**), or with Flt3L, GM-CSF or M-CSF as indicated and analyzed 1 d (**c**) and 3 d and 6 d (**d,f**) later by phase-contrast microscopy in cell culture (**c,d**) or after cytospin and May-Grünwald–Giemsa staining by bright-field microscopy (**e,f**). Unfractionated BM cells were cultured in parallel for 6 d under the same conditions. Scale bars, 50 μm (**c,d**) and 20 μm (**e,f**).
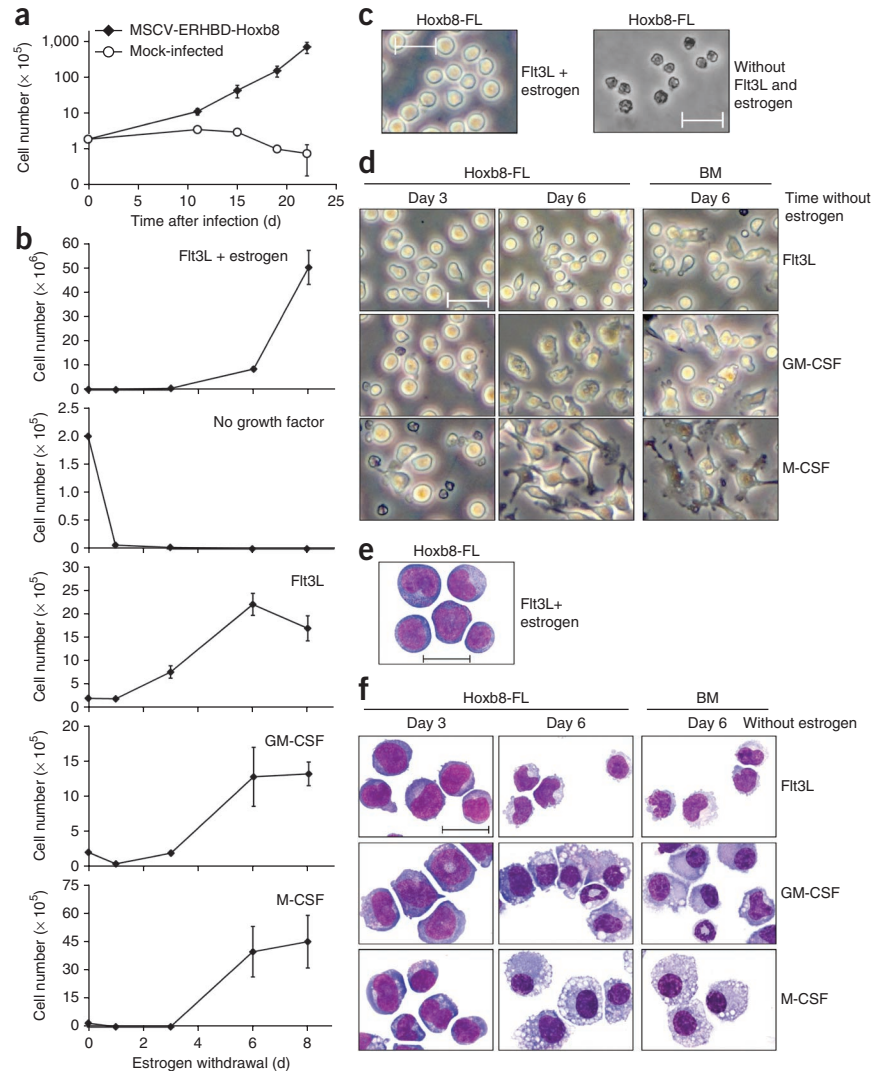
on nondifferentiated Hoxb8-FL cells (**Figs. 1c–f** and **2a,b**). On day 6, cells exhibited the typical phenotype of Flt3L-derived dendritic cells, that is, a biphenotypic population of so-called conventional dendritic cells (cDCs; CD11b⁺CD11c⁺MHC class II⁺B220⁻PDCA1⁻) and plasmacytoid dendritic cells (pDCs; CD11b⁻CD11c⁺B220⁺PDCA1⁺; **Fig. 2a,c** and **Supplementary Fig. 2**).

The Hoxb8-FL–derived cell population did not contain GR1^high CD11c⁻ granulocytes, which are contained in the input population of unfractionated BM and are only gradually lost during *in vitro* cell culture (**Fig. 2a**). Treatment of Hoxb8-FL– and BM–derived dendritic cells with known maturation factors, such as the TLR9 agonist CpG-DNA, led to strong upregulation of typical dendritic cell maturation markers, such as MHC class II, CD86 (B7.2) and CD40 (**Fig. 2d** and data not shown)[6]. Two major subtypes of splenic cDCs have been characterized: CD8⁻ and CD8⁺ dendritic cells, which correspond to *in vitro*–generated, Flt3L-driven CD11c⁺CD172a⁺CD24^low cells ('equivalent' eCD8⁻ dendritic cells) and CD11c⁺CD172^low CD24^high cells (eCD8⁺ dendritic cells), respectively[7]. More detailed flow cytometry analysis demonstrated that Hoxb8-FL cells indeed generated these dendritic cell subtypes, comparable to primary BM cells (**Fig. 2e**).

To test whether Hoxb8-FL cells have myeloid potential beyond the dendritic cell lineage, we replaced Flt3L upon estrogen removal with GM-CSF or M-CSF, which support *in vitro* the generation of dendritic cells and granulocytes, and macrophages, respectively. After a short period of less cell growth and limited cell death upon withdrawal of estrogen, both cytokines supported survival, expansion and eventually the generation of viable populations of differentiated cells (**Fig. 1b,d,f**). Cell differentiation became morphologically apparent after ~3 d (**Fig. 1d,f**). At day 6, GM-CSF–driven Hoxb8-FL cells exhibited the classic phenotype of GM-CSF–driven BM cells, characterized by a mixed population of dendritic cells (CD11b⁺CD11c⁺MHC class II⁺B220⁻) and

granulocytes (GR1^high CD11c⁻MHC class II⁻; **Fig. 2a,c**). In contrast, M-CSF–cultured Hoxb8-FL cells exhibited the characteristic adherent morphology of macrophages with the typical surface expression of CD11b and lack of MHC class II and GR1 (**Fig. 1d,f** and **Supplementary Fig. 3**). Similar to the Flt3L cultures, BM–derived cells still contained a small population of granulocytes (CD11b⁺GR1⁺MHC class II⁻; **Supplementary Fig. 3**). Taken together, these data indicate that Hoxb8-FL cells have the potential to differentiate into the major myeloid cell lineages.

Immune functions of Hoxb8-FL–derived myeloid cells

We analyzed key immune functions of Hoxb8-FL–derived myeloid cell types. Upon CpG-DNA–mediated activation of TLR9, B220⁺ pDCs produced robust amounts of interferon alpha (IFNα), whereas cDCs preferentially expressed interleukin 12 (IL-12) p40, both of which are key characteristics of the respective cell types[8] (**Fig. 2f**). Similarly, GM-CSF–driven, Hoxb8-FL–derived dendritic cells produced large amounts of IL-6 and IL-12 upon stimulation with CpG-DNA and lipopolysaccharide (**Supplementary Fig. 4**).

We exposed Hoxb8-FL–derived and BM-derived eCD8⁻ and eCD8⁺ cDCs to soluble ovalbumin as a model antigen, followed by incubation with ovalbumin-specific, MHC class II–restricted

Figure 2 | Phenotype and function of Hoxb8-FL–derived myeloid cells. (**a–c**) Flow cytometry analysis of Hoxb8-FL cells or BM cells after 3 d and 6 d (**a,b**) and after 6 d (**c**) of culture in the presence of Flt3L or GM-CSF. Day 0 corresponds to cells before differentiation. MHCII, major histocompatibility class II. Numbers in quadrants indicate percentages of cells. (**d**) Flow cytometry analysis of cells differentiated with Flt3L for 6 d, followed by treatment with (open) or without (filled) CpG-DNA for 18. (**e**) Flow cytometry analysis of cells differentiated with Flt3L for 10 d. (**f**) Flow cytometry analysis of Hoxb8-FL cells differentiated with Flt3L for 6 d, treated with (CpG) or without (ctrl) CpG-DNA followed by intracellular cytokine staining. (**g**) OTII and OTI T-cell proliferation in the absence (filled) or presence of dendritic cells (open) derived from Hoxb8-FL cells or BM cells after differentiation with Flt3L for 9 d (Online Methods). (**h**) Percentage of mice with tumors smaller than 1 cm^3 analyzed over time after immunization with ovalbumin-pulsed DCs and challenge 1 week later with B16 melanoma cells. $*P < 0.05$; $**P < 0.003$ (log-rank test; $n = 5$ mice per group). (**i**) Nitrate amounts in the supernatants of cells differentiated with M-CSF and treated with lipopolysaccharide (LPS) and IFNγ. Error bars, s.d. ($n = 3$ wells). (**j**) Uptake of IgG-coated beads by cells differentiated with M-CSF and incubated with beads at 37 °C for 2 h (solid) or 6 h (thick line) or at 4 °C for 6 h (thin line).

or MHC class I–restricted T-cell receptor (TCR) transgenic T cells, that is, OTII and OTI T cells[9,10], respectively. Hoxb8-FL–derived eCD8$^-$ cDCs triggered proliferation of OTII T cells, whereas eCD8$^+$ cDCs induced proliferation of OTI T cells, comparable to BM–derived dendritic cells (**Fig. 2g**). Finally, we compared immunogenicity of Hoxb8-FL–derived and BM-derived dendritic cells in an antigen (ovalbumin)-specific B16 melanoma model. Dendritic cells from both sources induced robust OTII and OTI T-cell activation *in vitro* (**Supplementary Fig. 5**) and, upon vaccination of mice, protected the mice from tumors developed from B16 cells transplanted 1 week after vaccination (**Fig. 2h**).

We tested release of nitric oxide and phagocytosis to evaluate macrophage function. M-CSF–driven, Hoxb8-FL–derived macrophages produced nitric oxide upon treatment with lipopolysaccharide and IFNγ in amounts that were virtually indistinguishable from those in their primary cell counterparts (**Fig. 2i**) and also phagocytosed comparable amounts of immunoglobulin G (IgG)-coated beads (**Fig. 2j**). Thus, Hoxb8-FL–derived dendritic cells and macrophages correspond functionally to BM–derived primary cells.

Myeloid and lymphoid potential *in vivo*

Given the known activity of Flt3L on very early hematopoietic progenitor cells, we defined the lineage potential of Hoxb8-FL cells *in vivo*[4,11]. We transferred Hoxb8-FL cells into lethally irradiated mice and analyzed the appearance of mature cell types in the peripheral blood, also in comparison to cell lines dependent
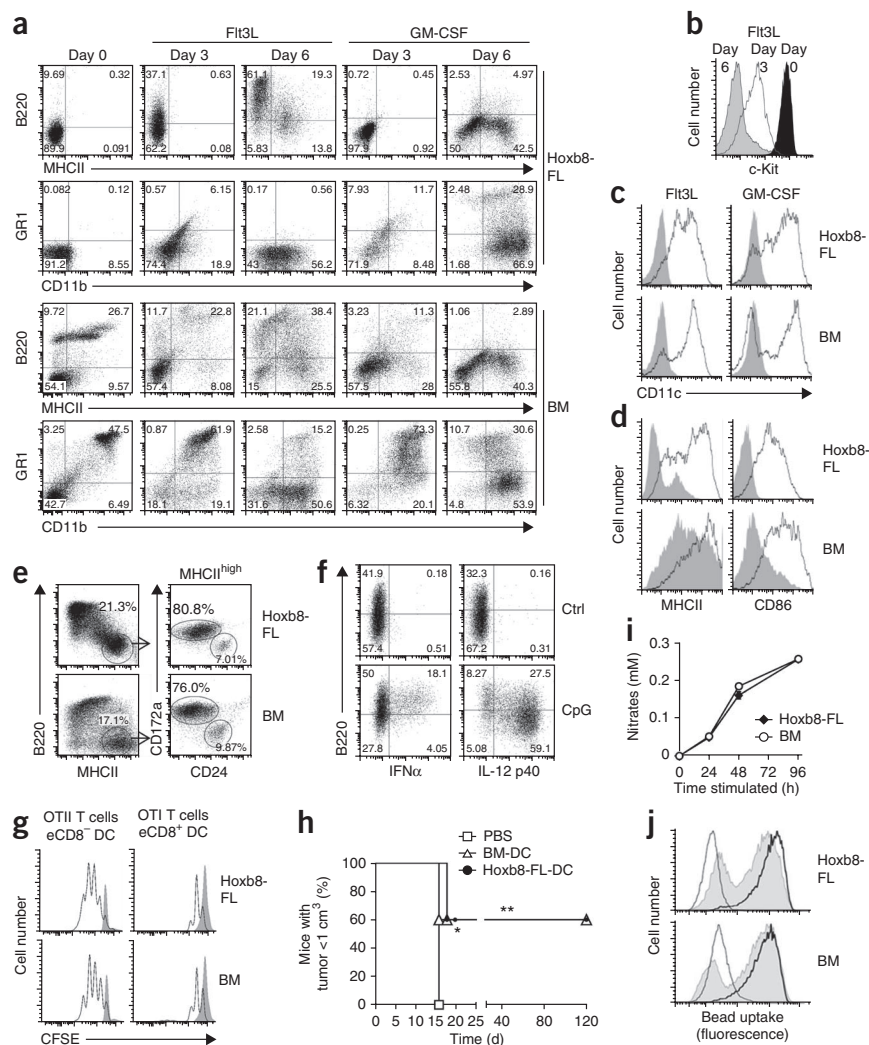
on Hoxb8 and SCF (Hoxb8-SCF), whose lineage potential has only been investigated *in vitro*[3]. Consistent with the *in vitro* data, Hoxb8-SCF cells generated only CD11b$^+$ myeloid cells, most of which were GR1^{high} granulocytes (**Fig. 3a** and **Supplementary Fig. 6a**), which were largely lost 1 week later. In contrast, Hoxb8-FL cells generated a mixed population of CD11b$^+$ cells, containing GR1^{high} granulocytes and at least two additional populations with GR1 intermediate (GR1^{int}) and GR1$^-$ phenotype (**Supplementary Fig. 6a**). The latter population was still detectable 14 d after transfer but was largely absent at day 28 (**Fig. 3a** and **Supplementary Fig. 6a,b**). Hoxb8-FL cells also generated B220$^+$CD11b$^-$CD11c$^-$ B lymphocytes and CD3$^+$ T lymphocytes, detectable 14 d and 28 d after transfer, respectively (**Fig. 3a** and **Supplementary Fig. 6b**).

We transferred Hoxb8-FL cells into lethally irradiated mice and analyzed their progeny in BM, spleen, blood and thymus at various time points. Two days after transfer, Hoxb8-FL–derived cells were detectable in high numbers in the BM and spleen but not in peripheral blood and thymus, and were largely negative for cell-lineage markers (**Supplementary Fig. 7**, **Fig. 3b–e** and data not shown). At day 6, CD11b$^+$ myeloid cells dominated in BM, spleen and peripheral blood, and a smaller population of B220$^+$ (CD11c$^-$) B-cell progenitors appeared in the BM (**Fig. 3b–d** and data not shown), which segregated almost exclusively into the Hardy fractions A and B of early B-cell

Figure 3 | *In vivo* differentiation of Hoxb8-FL cells. (**a**) Cell numbers over time of CD11b+, B220+ and CD3+ cells in the peripheral blood of lethally irradiated mice transplanted with Hoxb8-FL or Hoxb8-SCF cells. Error bars, s.d. (*n* = 3 mice). (**b–f**) Flow cytometry analysis of cells from BM (**b**), spleen (**c**), peripheral blood (**d**) and thymus (**e**) after Hoxb8-FL cells were transferred into lethally irradiated mice (shown data are representative of data obtained from six mice transferred with two independent Hoxb8-FL cell populations (three mice each per population) per time point). Tissue from untreated control mice (ctrl) was used for comparison. Numbers in quadrants indicate percentages of cells; some quadrants contain additional small gates. (**f**) Relative numbers of cells of the B-cell lineage in the BM and spleen (**Supplementary Fig. 8a**,**b**). A–F, Hardy fractions A–F of B-cell progenitors; T1–T3, transitional B-cell stages 1–3; Fo, follicular B cells; MZ, marginal zone B cells. Error bars for Hoxb8-FL–derived cells, s.d. of six mice that were transferred with two populations of Hoxb8-FL cells (three mice each). Error bars for untreated mice, s.d. (*n* = 6 mice).
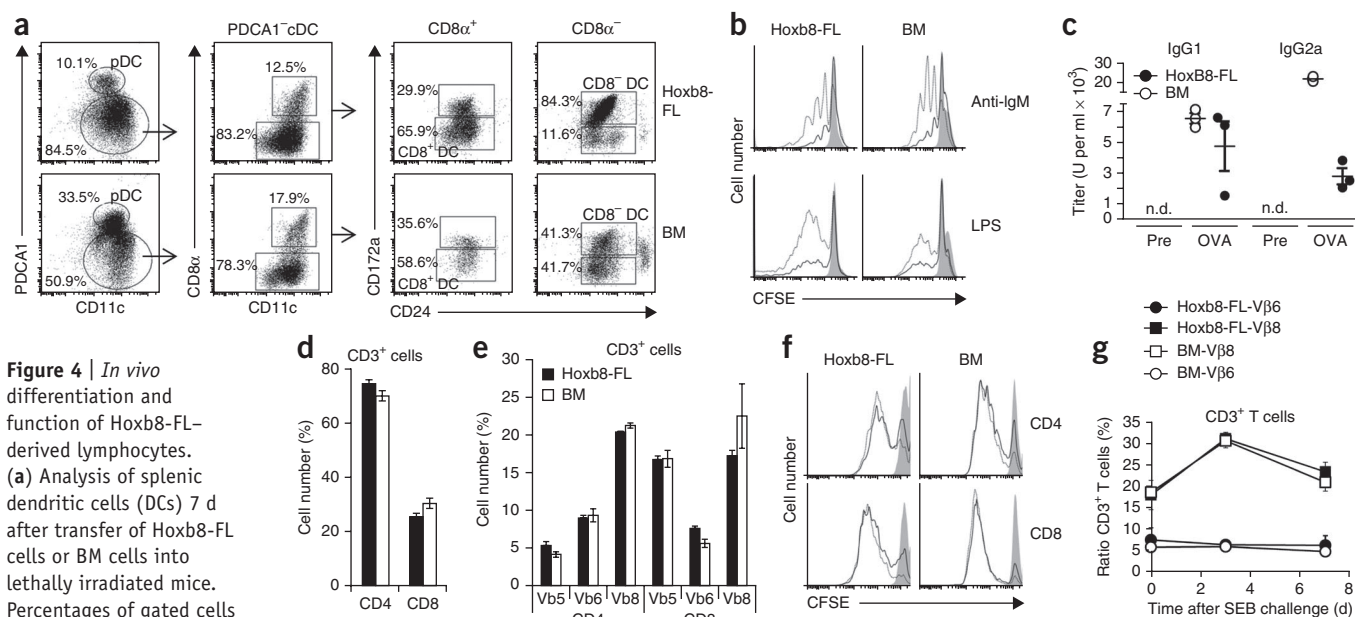

progenitors (**Fig. 3f**; for B-cell gating strategy, see **Supplementary Fig. 8a**,**b**)[12]. We found a small number of Hoxb8-FL–derived cells in the thymus at this time point. These cells, however, expressed CD11c and in part PDCA1, suggesting the migration of Hoxb8-FL–derived dendritic cells to the thymus rather than settling of the thymus with T-cell progenitors (**Fig. 3e**). At day 13, BM, spleen and peripheral blood were dominated by cells belonging to the B-cell lineage, whereas myeloid cells were merely detectable in the BM, and were detectable at low numbers in spleen, peripheral blood and thymus (**Fig. 3b–e**). B cells in the BM segregated mostly into Hardy fraction D, and those in the spleen largely had the phenotype of transitional T1 and T2 cells (**Fig. 3f**).

The majority of Hoxb8-FL–derived cells at day 13 in the thymus displayed a lineage marker–negative, CD4−CD8−CD25−CD44+ phenotype, characteristic of early thymus settling, CD4−CD8− cells (**Fig. 3e** and **Supplementary Fig. 9**). At day 22, the BM contained only a small number of Hoxb8-FL–derived cells, which were identified almost exclusively as fraction F (follicular) B cells (**Supplementary Fig. 7** and **Fig. 3f**). Likewise, the spleen contained primarily follicular B cells, and some T2 and T3 transitional B cells (**Fig. 3c**,**f**). We found no T cells in the periphery at day 22, but the thymus contained T cells resembling the steady state of physiological development of T cells, that is, CD4+CD8+ cells, mature CD4+ and CD8+ cells, and a smaller number of CD4−CD8− cells of all stages (1–4; **Fig. 3e** and **Supplementary Fig. 9**). At day 38, Hoxb8-FL cells had largely left the BM but were still present in spleen, peripheral blood and
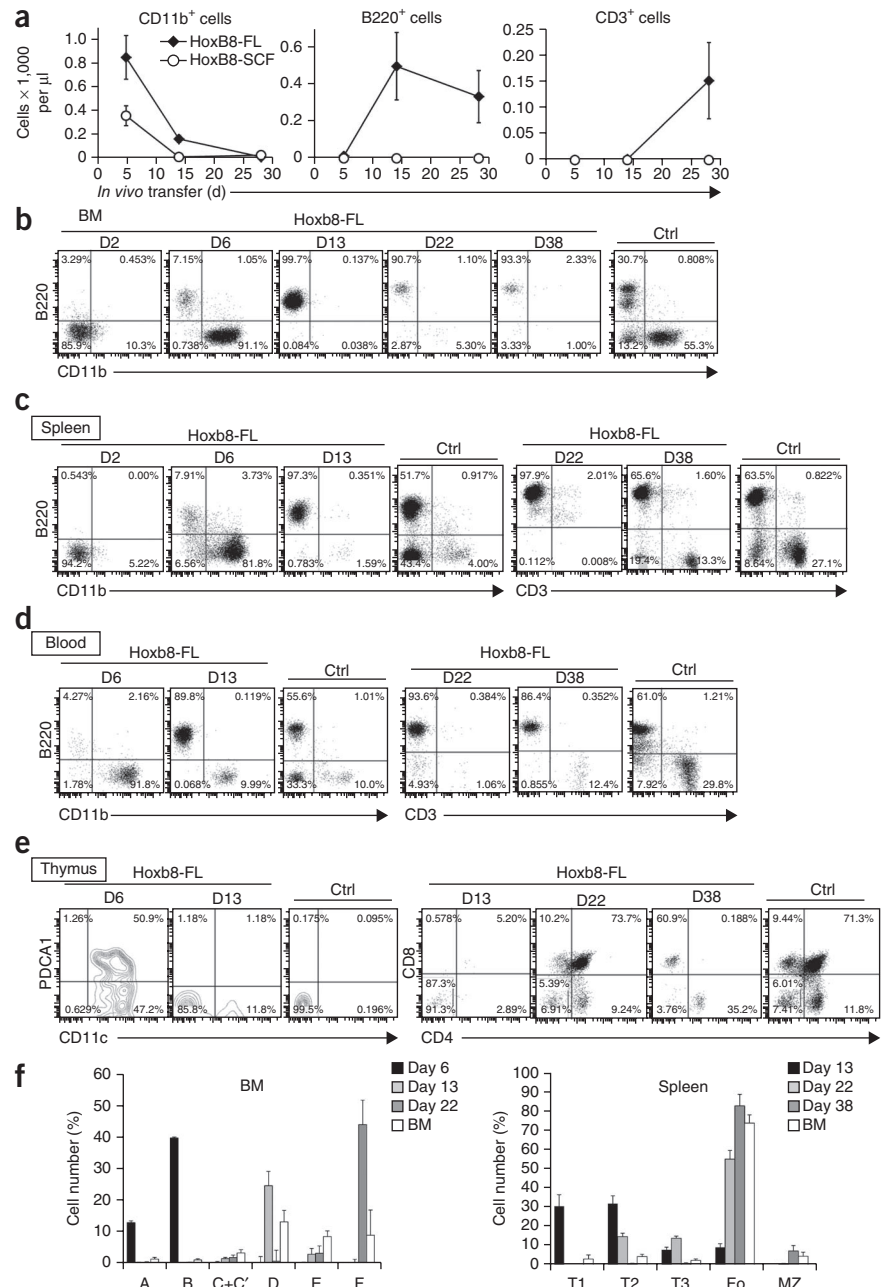
thymus (**Supplementary Fig. 7**). Splenic B cells had matured into follicular and marginal-zone B cells (**Fig. 3f**). Residual Hoxb8-FL–derived cells in the thymus displayed the mature phenotype of CD4+ or CD8+ thymocytes, and we also identified mature T cells in spleen and peripheral blood (**Fig. 3d**,**e**). In contrast to myeloid cells and B cells, Hoxb8-FL–derived T cells reached only about 10–30% of the number of T cells in untreated mice (**Fig. 3a**). This was not due to the irradiation protocol, which is known to influence maturation of T cells[13], as transfer of Hoxb8-FL cells into non-irradiated IL-7R–deficient mice, which can support development of T cells without conditioning irradiation, exhibited comparably low reconstitution of T cells (**Supplementary Fig. 10a**,**b**)[14].

Taken together, Hoxb8-FL cells have myeloid and lymphoid potential, which they realize *in vivo* in a time-dependent manner.

Figure 4 | *In vivo* differentiation and function of Hoxb8-FL–derived lymphocytes. (**a**) Analysis of splenic dendritic cells (DCs) 7 d after transfer of Hoxb8-FL cells or BM cells into lethally irradiated mice. Percentages of gated cells are indicated. (**b**) Flow cytometry analysis of splenocytes that were carboxyfluorescein diacetate succinimidyl ester (CFSE)-labeled and left untreated (filled) or stimulated for 3 d with anti-IgM (1 µg ml⁻¹ (solid line), 10 µg ml⁻¹ (dashed line)) or lipopolysaccharide (LPS; 0.1 µg ml⁻¹ (solid line), 0.5 µg ml⁻¹ (dashed line) 7 weeks after Hoxb8-FL cells and unfractionated BM cells were transferred into irradiated mice. CFSE signal correlates with the number of cell divisions and reflects cell proliferation. (**c**) Serum IgG1 and IgG2a antibody titers determined by enzyme-linked immunosorbent assay 1 d before immunization (Pre) and 10 d after the last immunization by intradermal injection of ovalbumin plus CpG-DNA (OVA) of mice transplanted with the indicated cells. n.d., not detectable. (**d**,**e**) Percentage of CD3⁺CD4⁺ and CD3⁺CD8⁺ splenocytes (**d**), and the distribution of select TCR Vβ chains on CD3⁺CD4⁺ and CD3⁺CD8⁺ splenocytes (**e**) analyzed 7 weeks after transplant of the indicated cells. Error bars, s.d. of three Hoxb8-FL populations. (**f**) Splenocytes described in **d**,**e** were CFSE labeled, stimulated for 2 d with plate-bound CD3 antibodies (10 µg ml⁻¹, dashed line; 3 µg ml⁻¹, solid line; nonstimulated, filled) and CD28 antibodies (10 µg ml⁻¹) and analyzed by flow cytometry. (**g**) Percentage of CD45.1⁺CD3⁺ T cells and CD45.2⁺CD3⁺ T cells expressing TCR Vβ6 and TCR Vβ8 chains in the peripheral blood before, 3 d after and 7 d after challenge with staphylococcal enterotoxin B (SEB), 5 weeks after CD45.1⁺ Hoxb8-FL cells and CD45.2⁺ BM cells were transferred into lethally irradiated mice. Mean and s.d. of four mice are shown.

The loss of immature cells over time strongly suggests that Hoxb8-FL cells do not have self-renewal capacity.

Characterization of Hoxb8-FL–derived immune cells
To test whether Hoxb8-FL cells realize the potential to differentiate into dendritic cells *in vivo*, we transferred Hoxb8-FL cells or unfractionated BM cells for comparison into lethally irradiated mice and purified CD11c⁺ and PDCA1⁺ cells from the spleen. Flow cytometry analysis showed that Hoxb8-FL cells gave rise to defined dendritic cell types comparable to BM, that is, pDCs, CD8⁺ cDCs and CD8⁻ cDCs (**Fig. 4a**).

We also characterized mature HoxB8-FL–derived B cells and T cells and found that, comparable to the case in BM-derived B cells, antibody-mediated cross-linking of B-cell receptors or stimulation with TLR agonists induced cell proliferation *in vitro* (**Fig. 4b**). To analyze function of B cells *in vivo*, we transferred Hoxb8-FL cells, or unfractionated BM cells, into lethally irradiated B cell–deficient (µMT) mice, followed by immunization with ovalbumin and immunostimulatory CpG-DNA. Serum collected from Hoxb8-FL–reconstituted mice contained robust amounts of ovalbumin-specific IgG1 and IgG2a (**Fig. 4c**), although IgG2a was less strongly induced than in mice reconstituted with unfractionated BM cells.

Analysis of Hoxb8-FL–derived T cells 5 weeks after transfer revealed an almost identical distribution of CD4⁺ and CD8⁺ cells as BM-derived T cells (**Fig. 4d**). Also, the repertoire of TCR variable β-chains (TCR Vβ) was very similar between Hoxb8-FL–derived and BM–derived T cells, as was the proliferative response upon antibody-mediated TCR cross-linking and CD28 stimulation *in vitro*, at least at high antibody concentrations (**Fig. 4e,f**). We also transferred Hoxb8-FL cells and unfractionated BM cells into lethally irradiated mice, followed by *in vivo* challenge with staphylococcal enterotoxin B, which activates selectively TCR Vβ8⁺ T cells. Three days after challenge with staphylococcal enterotoxin B, the pool of Hoxb8-FL– and BM–derived TCR Vβ8⁺ T cells expanded in number about twofold and diminished ('contracted') to close to baseline numbers 4 d later (**Fig. 4g**). T cells expressing TCR Vβ6⁺ were not affected, as expected. Thus, Hoxb8-FL–derived T cells exhibit the typical biology of antigen-specific populations of T cells *in vivo*.

Taken together, Hoxb8-FL cells differentiate *in vivo* into the major splenic dendritic cell populations and into lymphocytes that correspond phenotypically and functionally to primary BM–derived cells.

Potential to differentiate into lymphoid cells *in vitro*
Tissue-specific lymphocyte development can be recapitulated *in vitro* using described culture conditions that involve culture with stromal cell lines, for example, OP9 cells[15,16]. To test whether we could observe this for Hoxb8-FL cells, we cultured Hoxb8-FL cells together with OP9 cells and OP9 cells expressing the Notch ligand Delta-like 1 (OP9-DL1), and analyzed their phenotype over time.

Nondifferentiated Hoxb8-FL cells expressed high levels of CD44 but low or undetectable levels of CD25, B220 and Thy1 (**Fig. 5a**).
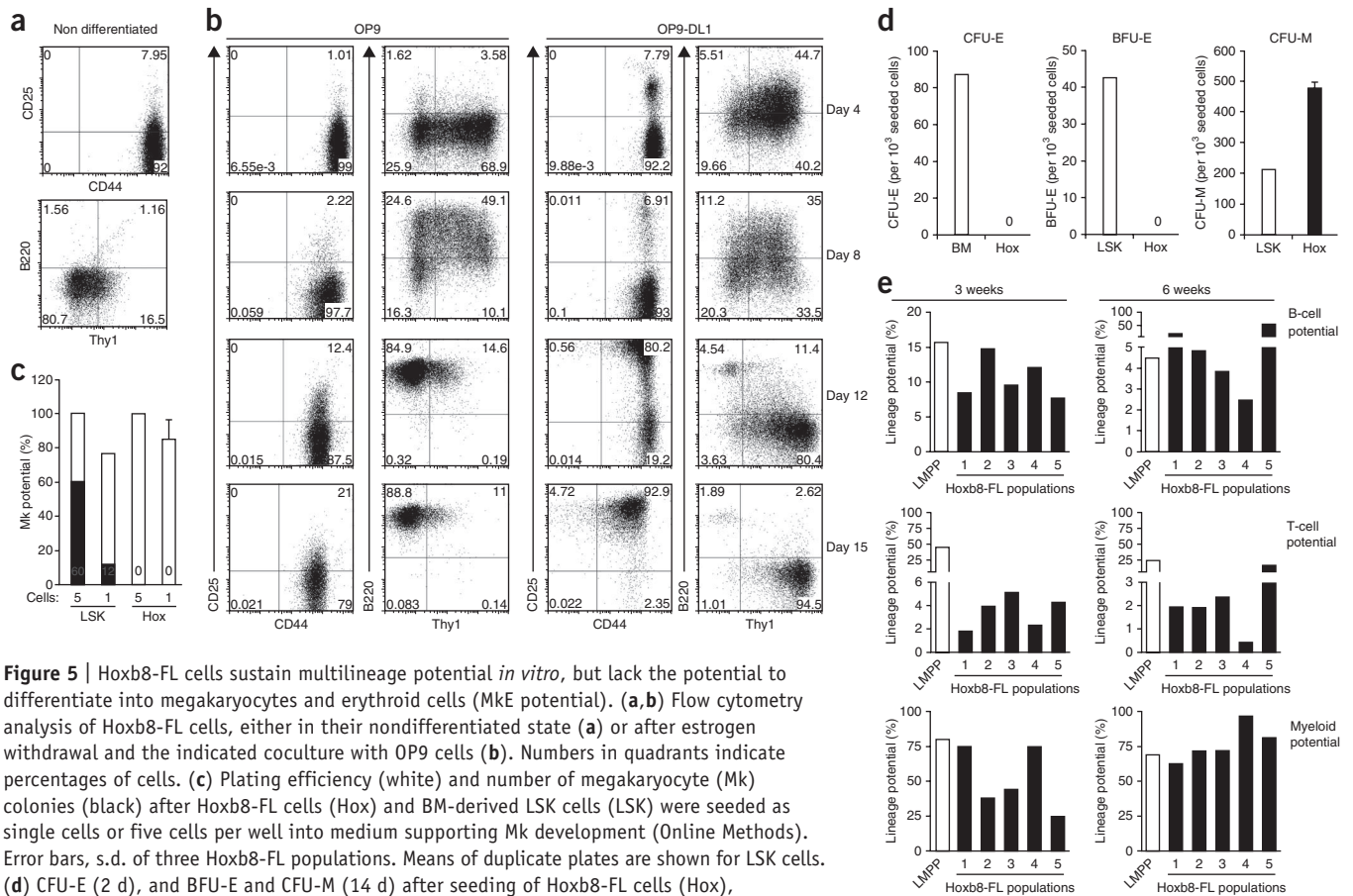
Figure 5 | Hoxb8-FL cells sustain multilineage potential *in vitro*, but lack the potential to differentiate into megakaryocytes and erythroid cells (MkE potential). (**a**,**b**) Flow cytometry analysis of Hoxb8-FL cells, either in their nondifferentiated state (**a**) or after estrogen withdrawal and the indicated coculture with OP9 cells (**b**). Numbers in quadrants indicate percentages of cells. (**c**) Plating efficiency (white) and number of megakaryocyte (Mk) colonies (black) after Hoxb8-FL cells (Hox) and BM-derived LSK cells (LSK) were seeded as single cells or five cells per well into medium supporting Mk development (Online Methods). Error bars, s.d. of three Hoxb8-FL populations. Means of duplicate plates are shown for LSK cells. (**d**) CFU-E (2 d), and BFU-E and CFU-M (14 d) after seeding of Hoxb8-FL cells (Hox), unfractionated BM (BM) or LSK cells (LSK) in methylcellulose containing supplemented medium (Online Methods). Error bars, s.d. of three Hoxb8-FL populations. Means of duplicate wells are shown for BM and LSK. (**e**) Lineage potential of five independent Hoxb8-FL cell populations and one LMPP cell population, analyzed after 3 weeks and 6 weeks of continuous *in vitro* culture.

After 4 d of culture of Hoxb8-FL cells with OP9 or OP9-DL1 cells, Thy1 was upregulated. In case of Hoxb8-FL cell culture with OP9 cells, upregulation was transient and was followed by homogenous, high expression of B220, indicative of commitment to the B-cell lineage (**Fig. 5b**)[12]. In case of Hoxb8-FL cell culture with OP9-DL1 cells, Thy1 expression was sustained and increased over time, accompanied by strong upregulation of CD25, resulting in the typical phenotype of CD4−CD8− double-negative 2 (DN2) T-cell progenitors (**Fig. 5b** and data not shown)[17] with B-cell progenitors almost completely absent, as expected[18,19]. Under these culture conditions, DN2 T-cell progenitors did not mature further (**Supplementary Fig. 11a** and data not shown). However, when adoptively transferred into lethally irradiated mice, the cells matured into CD3+CD4+ and CD3+CD8+ T cells (**Supplementary Fig. 11b**). The cells also generated CD11b+ myeloid cells, but not B220+ B cells, consistent with recent reports[20–22] (**Supplementary Fig. 11b**). Thus, Hoxb8-FL cells recapitulate early phases of development of B cells and T cells *in vitro*.

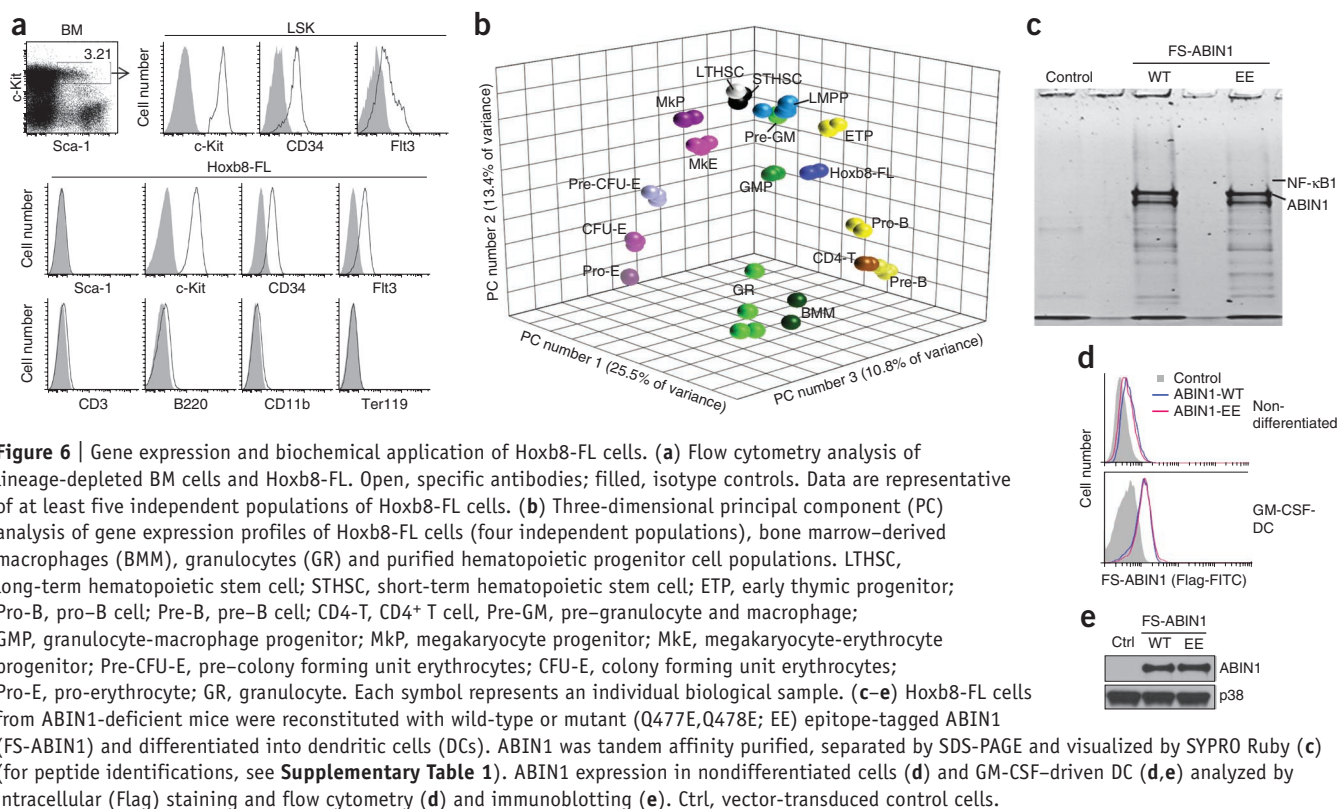**Quantitative analysis of lineage potential of Hoxb8-FL cells**

The decline of Hoxb8-FL–derived immune cells *in vivo* strongly suggests that the cells lack the capacity for self-renewal, indicating that they are a functional equivalent of multipotent progenitor (MPP) cells or lymphoid-primed MPP (LMPP) cells, the latter being defined as committed progenitor with myeloid and

lymphoid potential, but loss of the potential to differentiate into megakaryocytes and erythroid cells (megakaryocyte and erythroid potential)[23,24]. Using lineage marker–negative, Sca-1+c-Kit+ (LSK) cells and unfractionated BM cells as positive controls, we tested the potential of Hoxb8-FL cells to differentiate into megakaryocytes and erythroid cells (MkE lineage). Hoxb8-FL cells had neither the potential to differentiate into megakaryocytes (**Fig. 5c**), nor did they give rise to erythrocyte colony-forming units (CFU-E) or erythrocyte burst-forming units (BFU-E) in the presence of erythropoietin (**Fig. 5d**). Under conditions that additionally support myeloid development, Hoxb8-FL cells formed exclusively macrophage colony-forming units (CFU-M), whereas LSK cells formed CFU-M in addition to CFU-E and BFU-E, as expected (**Fig. 5d**). Hoxb8-FL cells thus functionally resemble LMPP cells.

Stability and homogeneity of Hoxb8-FL cells

To test the stability and homogeneity of Hoxb8-FL cells, we generated five independent Hoxb8-FL populations, cultured them continuously for 6 weeks, and determined their lineage potential after 3 weeks and 6 weeks by clonal assays (for myeloid potential) and limiting dilution assays (for B-cell and T-cell potential). BM-derived LMPP cells served as control. Three-week-old cultures exhibited a potential to differentiate into B cells and myeloid cells that was comparable to that of LMPP cells and also comparable

Figure 6 | Gene expression and biochemical application of Hoxb8-FL cells. (**a**) Flow cytometry analysis of lineage-depleted BM cells and Hoxb8-FL. Open, specific antibodies; filled, isotype controls. Data are representative of at least five independent populations of Hoxb8-FL cells. (**b**) Three-dimensional principal component (PC) analysis of gene expression profiles of Hoxb8-FL cells (four independent populations), bone marrow–derived macrophages (BMM), granulocytes (GR) and purified hematopoietic progenitor cell populations. LTHSC, long-term hematopoietic stem cell; STHSC, short-term hematopoietic stem cell; ETP, early thymic progenitor; Pro-B, pro–B cell; Pre-B, pre–B cell; CD4-T, CD4+ T cell; Pre-GM, pre–granulocyte and macrophage; GMP, granulocyte-macrophage progenitor; MkP, megakaryocyte progenitor; MkE, megakaryocyte-erythrocyte progenitor; Pre-CFU-E, pre–colony forming unit erythrocytes; CFU-E, colony forming unit erythrocytes; Pro-E, pro-erythrocyte; GR, granulocyte. Each symbol represents an individual biological sample. (**c–e**) Hoxb8-FL cells from ABIN1-deficient mice were reconstituted with wild-type or mutant (Q477E,Q478E; EE) epitope-tagged ABIN1 (FS-ABIN1) and differentiated into dendritic cells (DCs). ABIN1 was tandem affinity purified, separated by SDS-PAGE and visualized by SYPRO Ruby (**c**) (for peptide identifications, see **Supplementary Table 1**). ABIN1 expression in nondifferentiated cells (**d**) and GM-CSF–driven DC (**d,e**) analyzed by intracellular (Flag) staining and flow cytometry (**d**) and immunoblotting (**e**). Ctrl, vector-transduced control cells.

among the different populations (**Fig. 5e**). B-cell potential and myeloid potential were preserved after 6 weeks of culture, although we observed some variability in the former (**Fig. 5e**). Hoxb8-FL populations had homogenous potential to differentiate into T cells, about tenfold lower than that of LMPP cells. Potential to differentiate into T cells was also preserved after 6 weeks of culture.

To evaluate the homogeneity of the cell populations generated by this approach, we subcloned four populations and tested the lineage potential of four of these clones in quantitative assays after 6 weeks of culture. All clones exhibited relatively homogenous B-cell potential and myeloid potential, comparable to that of the original populations and close to that of LMPP cells (**Supplementary Fig. 12**). With the exception of two clones, clones had the same or even greater T-cell potential (**Supplementary Fig. 12**). Thus, Hoxb8-FL cells are a homogenous population of cells that maintain multilineage potential stably over a period of at least 6 weeks.

Phenotype and gene expression analysis of Hoxb8-FL cells

Comparable to LMPP cells[23], Hoxb8-FL cells are negative for hematopoietic lineage markers and homogenously express c-Kit, Flt3 and CD34; in contrast to LMPP cells, however, Hoxb8-FL cells do not express detectable levels of SCA-1 (**Fig. 6a**). To refine the relation of Hoxb8-FL cells to other hematopoietic cells, we performed microarray-based genome-wide expression analyses, defined cell type–specific gene expression profiles by analysis of variance (ANOVA) and visualized those profiles by principal component analysis (PCA). The four independent Hoxb8-FL cell populations clustered closely together, reflecting their molecular similarity, but were distant from the erythroid and megakaryocytic

lineage and also distant from mature immune cells (**Fig. 6b**). Although Hoxb8-FL cells also cluster distantly from hematopoietic stem cells and somewhat closer to LMPP cells (particularly in the first principal component), they cluster in between myeloid and lymphoid branches as extending from LMPP cells to granulocyte-macrophage progenitor cells and myeloid cells, and from LMPP cells to early thymic progenitor cells and lymphoid cells, respectively.

Proteomic analysis of Hoxb8-FL–derived dendritic cells

Hoxb8-FL cells should prove invaluable in experimental settings that require large numbers of rare cells. For instance, proteomic analysis of dendritic cells from ABIN1-deficient mice, which largely die during embryonic development, is not feasible or is very difficult using current technologies[25,26]. ABIN1 is a ubiquitin-binding protein with functions in many pathways[25–27], but its molecular mechanism, particularly in immune cells, is largely unclear. To identify ABIN1-interacting proteins, we generated Hoxb8-FL cells from BM of ABIN1-deficient mice and introduced, by retroviral transduction, sequences encoding wild-type ABIN1 and a ubiquitin-binding mutant (ABIN1(Q477E,Q478E)), each containing triple Flag and One-STrEP epitope tags. Stably growing, polyclonal populations and vector-transduced control cells were scaled up and differentiated into 8×10^8 dendritic cells in the presence of GM-CSF, followed by tandem affinity purification of ABIN1 and analysis of ABIN1-associated proteins by SDS-PAGE and liquid chromatography–coupled mass spectrometry (**Fig. 6c**). Both wild-type and mutant ABIN1 were stably and homogenously expressed during differentiation (**Fig. 6d,e**). We identified several ABIN1-interacting proteins, including NF-κB1 (p105), represented by a large number of unique peptides in both wild-type

ABIN1 and ABIN1(Q477E,Q478E) purified samples but not control samples (**Supplementary Table 1**). Overexpression of ABIN1 has been shown to counteract constitutive processing of NF-κB1 into its active form[28]. As such, our data confirm a physical interaction of ABIN1 and NF-κB1, and indicate a physiological function of ABIN1 in the NF-κB pathway in dendritic cells.

DISCUSSION

The method we described for generating mouse hematopoietic progenitor cell lines is remarkable in its simplicity, as it is based on largely unfractionated BM, standard retroviral transduction and cell culture techniques. We also generated similar cell lines with myeloid and lymphoid potential starting with LSK cells (**Supplementary Fig. 13**). We established more than 90 Hoxb8-FL cell lines, varying systematically different aspects of the procedure, including virus titer (multiplicity of infection of 1 to 100) and viral vector (MSCV versus lentivirus). Irrespective of the conditions used, the efficiency for generation of Hoxb8-FL cell lines was 100%, and the phenotype of all lines was uniform.

Hoxb8-FL cells resemble LMPP cells in phenotype and lineage potential but do not express SCA-1. Based on Pu.1-GFP reporter mice, it has been recently shown that LMPP cells express SCA-1 at the lower end of an expression spectrum of LSK cells, indicating a gradual loss of SCA-1 expression along with the loss of multilineage potential and commitment to immune cell lineages[29]. Hoxb8-FL cells may therefore be a cell type arising after strictly defined SCA-1^{+} LMPPs during lineage commitment. This interpretation is also consistent with their position in the PCA of gene expression patterns.

Hoxb8-FL cells had diminished T-cell potential *in vitro* and *in vivo*, but they generated B220^{+} B cells *in vivo* at numbers comparable to those for endogenous B cells (**Figs. 3a** and **5e** and **Supplementary Fig. 10**). One possible explanation is that Hoxb8-FL cells indeed have lower T-cell potential compared to LMPP cells but maintain the potential to differentiate into myeloid cells and B cells. This interpretation is less compatible with observations related to thymic lineage commitment, where potential to differentiate into B cells is diminished before restriction in the potential to differentiate into myeloid cells is apparent[20–22]. An alternative explanation in the *in vitro* context is that the specific OP9-DL1 coculture conditions, optimized for LMPP cells, may be not ideal for Hoxb8-FL cells. An alternative explanation for the relatively low number of T cells *in vivo* is the known limited access of the thymus for thymus-settling progenitor cells from the blood[30–33]. This is likely to be particularly relevant for Hoxb8-FL–derived cells, which are not replenished by self-renewal, thereby decreasing the temporal window of opportunity to enter the thymus. Hoxb8-FL cell–derived immature progenitor cells could be detected in the thymus at the earliest after day 6 of adoptive transfer, well after population of the BM, indicating that thymus settling occurs after and potentially via BM settling. This interpretation is consistent with data suggesting that Flt3^{+} MPP cells, which phenotypically overlap with LMPP cells, settle the thymus via the BM[34]. If so, the BM environment, which is particularly conducive to development of B cells, may additionally reduce the number of potentially thymus-settling Hoxb8-FL cell–derived progenitors.

Hoxb8-FL cells have a wide range of possible applications, such as the proteomic analysis of rare cell types we performed or the investigation of factors implicated in cell differentiation *in vitro* and *in vivo*.

METHODS

Methods and any associated references are available in the online version of the paper.

Accession code. Gene Expression Omnibus: GSE45759 (Affymetrix microarray data for Hoxb8-FL cells).

Note: Supplementary information is available in the online version of the paper.

AUTHOR CONTRIBUTIONS
V.R., R.W., V.C. and H.H. planned experiments; V.R., R.W., J.Z., V.C. and H.H. performed experiments; A.A.H., D.F., V.C., V.R. and H.H. analyzed data; V.R. and H.H. wrote the manuscript; and H.H. conceived the project.

1. Argiropoulos, B. & Humphries, R.K. Hox genes in hematopoiesis and leukemogenesis. *Oncogene* **26**, 6766–6776 (2007).
2. Pineault, N., Helgason, C.D., Lawrence, H.J. & Humphries, R.K. Differential expression of Hox, Meis1, and Pbx1 genes in primitive cells throughout murine hematopoietic ontogeny. *Exp. Hematol.* **30**, 49–57 (2002).
3. Wang, G.G. *et al.* Quantitative production of macrophages or neutrophils *ex vivo* using conditional Hoxb8. *Nat. Methods* **3**, 287–293 (2006).
4. McKenna, H.J. *et al.* Mice lacking flt3 ligand have deficient hematopoiesis affecting hematopoietic progenitor cells, dendritic cells, and natural killer cells. *Blood* **95**, 3489–3497 (2000).
5. Gilliet, M. *et al.* The development of murine plasmacytoid dendritic cell precursors is differentially regulated by Flt3-ligand and granulocyte/macrophage colony-stimulating factor. *J. Exp. Med.* **195**, 953–958 (2002).
6. Steinman, R.M. Dendritic cells: understanding immunogenicity. *Eur. J. Immunol.* **37** (suppl. 1), S53–S60 (2007).
7. Naik, S.H. *et al.* Cutting edge: generation of splenic CD8^{+} and CD8^{−} dendritic cell equivalents in Fms-like tyrosine kinase 3 ligand bone marrow cultures. *J. Immunol.* **174**, 6592–6597 (2005).
8. Hemmi, H., Kaisho, T., Takeda, K. & Akira, S. The roles of Toll-like receptor 9, MyD88, and DNA-dependent protein kinase catalytic subunit in the effects of two distinct CpG DNAs on dendritic cell subsets. *J. Immunol.* **170**, 3059–3064 (2003).
9. Hogquist, K.A. *et al.* T cell receptor antagonist peptides induce positive selection. *Cell* **76**, 17–27 (1994).
10. Barnden, M.J., Allison, J., Heath, W.R. & Carbone, F.R. Defective TCR expression in transgenic mice constructed using cDNA-based alpha- and beta-chain genes under the control of heterologous regulatory elements. *Immunol. Cell Biol.* **76**, 34–40 (1998).
11. Sitnicka, E. *et al.* Key role of flt3 ligand in regulation of the common lymphoid progenitor but not in maintenance of the hematopoietic stem cell pool. *Immunity* **17**, 463–472 (2002).
12. Hardy, R.R., Carmack, C.E., Shinton, S.A., Kemp, J.D. & Hayakawa, K. Resolution and characterization of pro-B and pre-pro-B cell stages in normal mouse bone marrow. *J. Exp. Med.* **173**, 1213–1225 (1991).
13. Zlotoff, D.A. *et al.* Delivery of progenitors to the thymus limits T-lineage reconstitution after bone marrow transplantation. *Blood* **118**, 1962–1970 (2011).

14. Prockop, S.E. & Petrie, H.T. Regulation of thymus size by competition for stromal niches among early T cell progenitors. *J. Immunol.* **173**, 1604–1611 (2004).

15. Carlyle, J.R. *et al.* Identification of a novel developmental stage marking lineage commitment of progenitor thymocytes. *J. Exp. Med.* **186**, 173–182 (1997).

16. Schmitt, T.M. & Zuniga-Pflucker, J.C. Induction of T cell development from hematopoietic progenitor cells by delta-like-1 *in vitro*. *Immunity* **17**, 749–756 (2002).

17. Godfrey, D.I., Kennedy, J., Suda, T. & Zlotnik, A. A developmental pathway involving four phenotypically and functionally distinct subsets of CD3–CD4-CD8- triple-negative adult mouse thymocytes defined by CD44 and CD25 expression. *J. Immunol.* **150**, 4244–4252 (1993).

18. Pui, J.C. *et al.* Notch1 expression in early lymphopoiesis influences B versus T lineage determination. *Immunity* **11**, 299–308 (1999).

19. Sultana, D.A., Bell, J.J., Zlotoff, D.A., De Obaldia, M.E. & Bhandoola, A. Eliciting the T cell fate with Notch. *Semin. Immunol.* **22**, 254–260 (2010).

20. Wada, H. *et al.* Adult T-cell progenitors retain myeloid potential. *Nature* **452**, 768–772 (2008).

21. Bell, J.J. & Bhandoola, A. The earliest thymic progenitors for T cells possess myeloid lineage potential. *Nature* **452**, 764–767 (2008).

22. Luc, S. *et al.* The earliest thymic T cell progenitors sustain B cell and myeloid lineage potential. *Nat. Immunol.* **13**, 412–419 (2012).

23. Adolfsson, J. *et al.* Identification of Flt3+ lympho-myeloid stem cells lacking erythro-megakaryocytic potential a revised road map for adult blood lineage commitment. *Cell* **121**, 295–306 (2005).

24. Yang, L. *et al.* Identification of Lin(–)Sca1(+)kit(+)CD34(+)Flt3– short-term hematopoietic stem cells capable of rapidly reconstituting and rescuing myeloablated transplant recipients. *Blood* **105**, 2717–2723 (2005).

25. Oshima, S. *et al.* ABIN-1 is a ubiquitin sensor that restricts cell death and sustains embryonic development. *Nature* **457**, 906–909 (2009).

26. Zhou, J. *et al.* A20-binding inhibitor of NF-kappaB (ABIN1) controls Toll-like receptor-mediated CCAAT/enhancer-binding protein beta activation and protects from inflammatory disease. *Proc. Natl. Acad. Sci. USA* **108**, E998–E1006 (2011).

27. Mauro, C. *et al.* ABIN-1 binds to NEMO/IKKgamma and co-operates with A20 in inhibiting NF-kappaB. *J. Biol. Chem.* **281**, 18482–18488 (2006).

28. Cohen, S., Ciechanover, A., Kravtsova-Ivantsiv, Y., Lapid, D. & Lahav-Baratz, S. ABIN-1 negatively regulates NF-kappaB by inhibiting processing of the p105 precursor. *Biochem. Biophys. Res. Commun.* **389**, 205–210 (2009).

29. Arinobu, Y. *et al.* Reciprocal activation of GATA-1 and PU.1 marks initial specification of hematopoietic stem cells into myeloerythroid and myelolymphoid lineages. *Cell Stem Cell* **1**, 416–427 (2007).

30. Wallis, V.J., Leuchars, E., Chwalinski, S. & Davies, A.J. On the sparse seeding of bone marrow and thymus in radiation chimaeras. *Transplantation* **19**, 2–11 (1975).

31. Spangrude, G.J. & Scollay, R. Differentiation of hematopoietic stem cells in irradiated mouse thymic lobes. Kinetics and phenotype of progeny. *J. Immunol.* **145**, 3661–3668 (1990).

32. Zlotoff, D.A. *et al.* CCR7 and CCR9 together recruit hematopoietic progenitors to the adult thymus. *Blood* **115**, 1897–1905 (2010).

33. Foss, D.L., Donskoy, E. & Goldschneider, I. The importation of hematogenous precursors by the thymus is a gated phenomenon in normal adult mice. *J. Exp. Med.* **193**, 365–374 (2001).

34. Serwold, T., Ehrlich, L.I. & Weissman, I.L. Reductive isolation from bone marrow and blood implicates common lymphoid progenitors as the major source of thymopoiesis. *Blood* **113**, 807–815 (2009).

ONLINE METHODS

Reagents and plasmids. Antibodies used were against B220 (RA3-6B2, dilution 1:200), CD4 (RM4-5, dilution 1:200), CD45.1 (A20, dilution 1:200), MHC class II (M5/114.15.2, dilution 1:300), GR1 (Ly6G (RB6-8C5), dilution 1:1,000), CD11c (N418, dilution 1:100), IgM (eB121-15F9, dilution 1:50), CD25 (PC61.5, dilution 1:500), CD44 (IM7, dilution 1:1,000), Thy1.2 (53-2.1, dilution 1:300), CD34 (RAM34, dilution 1:100), Flt3 (A2F10, dilution 1:50), Sca-1 (D7, dilution 1:100), Ter119 (TER-119, dilution 1:300), CD19 (1D3, dilution 1:100), AA4.1 (AA4.1, dilution 1:100), CD21 (ebio8D9, dilution 1:200), CD24 (30 -F1, for dendritic cells (DCs), dilution 1:200), CD24 (M1/69, for BM-B cells, dilution 1:400), CD172a (P84, dilution 1:50), IgD (11-26, dilution 1:200) (all from eBiosciences); CD3 (145-2C11, dilution 1:300), CD8α (53-6.7, dilution 1:200), CD11b (M1/70, dilution 1:200), CD11c (HL3, dilution 1:100), c -Kit (2B8, dilution 1:100), Sca-1 (E13-161.7, dilution 1:100), IL-12p40 (C15.6, dilution 1:100), CD43 (S7, dilution 1:25), BP-1 (6C3, dilution 1:100) (all from BD Biosciences); CD23 (30-F1, Genway, dilution 1:300), PDCA-1 (Miltenyi, dilution 1:25), IFNα (RMMA1, PBL, dilution 1:25) and ABIN1 (1A11E3, Invitrogen, dilution 1:1,000). Enzyme-linked immunosorbent assay (ELISA) kits for IL-6 and IL-12 were from BD Biosciences. Griess assays for determination of nitric oxide concentration were done as described[35]. CpG-DNA (TIB Molbiol) refers to the phosphothioate backbone containing oligonucleotides '1668' (1 μM, TCCATGACGTTCCTGATGCT), which was used in all assays with the exception of the experiment shown in **Figure 2f**, where '2216' (3 μM, GGGGGACGATCGTCGGGGGG) was used. Other agonists used were lipopolysaccharide (10 ng/ml, *Escherichia coli* 0127:B8 (Sigma-Aldrich)), IFNγ (10 ng/ml, Peprotech), β-estradiol (1 μM, Sigma-Aldrich). Recombinant mouse growth factors (SCF, Flt3L, TPO, IL-3, IL-6) were from Peprotech, human erythropoietin was from Amgen. Mouse *Hoxb8* cDNA was amplified by PCR using Wehi-3 cDNA as template and was cloned into MSCVneo (BD Biosciences) downstream of a triple hemagglutinin (HA) epitope tag. The sequence encoding the estrogen binding domain of the human estrogen receptor (ERHBD) was amplified by overlap extension PCR based on cDNA of the human estrogen receptor 1 (Open Biosystems, clone ID40128594), introducing the mutation that results in the characterized G400V substitution, which renders the hormone-binding domain insensitive to physiological concentrations of estrogen or phenol red contained in growth medium[36]. The mutagenized fragment encoding ERHBD was cloned in frame between sequence encoding the triple HA tag and *Hoxb8*, resulting in the final MSCV-ERHBD-Hoxb8 vector. The sequence of the expression cassette was confirmed by DNA sequencing.

Virus production. The plasmids MSCV-ERHBD-Hoxb8 and the ecotropic packaging vector pCL-Eco (Imgenex) were both transfected into HEK293T cells using Lipofectamine 2000 (Invitrogen). Eighteen hours after transfection, the supernatant was replaced by fresh growth medium (DMEM (Invitrogen), supplemented with 10% (v/v) FCS (Hyclone), 50 mM 2-mercaptoethanol, antibiotics (penicillin G (100 IU/ml) and streptomycin sulfate (100 IU/ml) and pyruvate (1 mM)), followed by incubation for 24 h and collection of virus-containing supernatant. Virus titers were determined on mouse embryonic fibroblast cells based on G418 resistance mediated by the retroviral vector.

Generation and cell culture of Hoxb8-FL and Hoxb8-SCF progenitor cell lines. BM cells were collected by flushing femurs of 4–8-week-old female C57BL/6J or B6.SJL mice with 10 ml RP-10 (RPMI 1640 (Invitrogen), supplemented with 10% (v/v) FCS (Hyclone), 50 mM 2-mercaptoethanol and antibiotics (penicillin G (100 IU/ml) and streptomycin sulfate (100 IU/ml))), pelleted by centrifugation, resuspended in 4 ml RP-10, loaded on 3 ml Ficoll-Paque (GE Healthcare) and separated by centrifugation at 450*g* for 30 min. The entire supernatant was collected (discarding only 500 μl including the cell pellet), diluted with 45 ml of PBS containing 1% fetal calf serum (FCS) (PBS containing FCS), pelleted at 800*g* for 10 min, followed by resuspension in 10 ml RP-10, centrifugation at 450*g* for 5 min and resuspension at a concentration of 5×10^5 cells/ml in RP-10 containing recombinant mouse IL-3 (10 ng/ml), IL-6 (20 ng/ml) and 1% of cell culture supernatant from a SCF-producing B16 melanoma cell line (provided by M. Kamps; University of California, San Diego), corresponding to the bioactivity of 250 ng/ml recombinant SCF (R&D Systems). After 2 d of cell culture, cells were collected, resuspended in progenitor outgrowth medium (POM), that is, RP-10 supplemented with 1 μM β-estradiol and either cell culture supernatant from an Flt3L-producing B16 melanoma cell line (provided by R. Steinman; Rockefeller University) for generation of Hoxb8-FL cells (5% final concentration) or the described SCF-producing cell line for generation of Hoxb8-SCF cells (1% final concentration). A total of 2×10^5 cells were dispensed in 1 ml per well in a 12-well plate and infected with MSCV vectors (multiplicity of infection, 5) by spin inoculation at 1,500*g* for 60 min in the presence of Lipofectamine (0.1%, Invitrogen). After infection, cells were diluted by adding 1.5 ml POM for 24 h, followed by removal and replacement of 2 ml of the cell culture medium. During the following cell culture period, cells were dispensed every 3–4 d in fresh medium and transferred into new wells. Once the cell populations were stably expanding, cells were kept at concentrations between 1×10^5 cells/ml medium and 1.5×10^6 cells/ml medium. For subsequent differentiation experiments, cells were washed twice with PBS containing FCS and resuspended in a concentration of 0.5×10^5–2×10^5 cells/ml in RP-10 containing specific growth factors as described for BM-derived DCs and macrophages. For *in vivo* experiments, 5×10^6 cells were resuspended in 0.2 ml PBS containing FCS (along with 2×10^5 unfractionated BM cells) and transferred into mice via tail-vein injection.

Phagocytosis assay. Hoxb8-FL cells and BM cells were differentiated in the presence of M-CSF contained in L-cell conditioned medium for 7 d, followed by incubation with FITC-labeled IgG-coated beads (1:100, Cayman Chemical, Phagocytosis kit (IgG FITC)) either at 37 °C or 4 °C for 2 h and 6 h. Cells were washed with PBS and trypsin, detached with trypsin and analyzed by flow cytometry.

Mice and transfer of Hoxb8-FL cells and BM cells into mice. All mouse studies were carried out in accordance with protocols approved by the Institutional Animal Care and Use Committee at St. Jude Children's Research Hospital. Four- to six-week-old female mice were used. After 5×10^6 CD45.1+ Hoxb8-FL cells (derived from B6/SJL mice), together with 2×10^5 CD45.2+ BM cells (derived from C57BL/6J mice), were collected by centrifugation,

they were resuspended in 200 µl PBS containing FCS and transferred via tail-vein injection into C57BL/6J wild-type, $Il7r^{-/-}$ or µMT mice (The Jackson Laboratory) that had been lethally irradiated at 950 rad 1 d before cell transfer where indicated in figure legends. Hoxb8-FL– and BM–derived cells were differentiated based on CD45.1 and CD45.2 staining. ABIN1-deficient mice, which were generated using embryonic stem cells obtained from the German Gene Trap Consortium, have been described[26]. Peripheral blood was collected by retro-orbital bleeding. Complete blood counts were measured using the Forcyte Hematology System (Oxford Science).

Mouse immunization and analysis of serum IgG titers. A total of 5×10^6 Hoxb8-FL cells or unfractionated BM cells were transferred into lethally irradiated µMT mice along with unfractionated 2×10^5 BM helper cells from µMT mice, followed by intradermal injection of ovalbumin (1 µg) plus CpG-DNA (50 µg) in 50 µl PBS at the base of the tail on days 21, 31 and 41 after transfer. Serum was collected 1 day before immunization and 10 d after the last immunization, and IgG1 and IgG2a antibody titers were determined by ELISA. Relative units were determined based on pooled, high-titer 'standard' serum obtained from wildtype mice that had been immunized with ovalbumin plus alum (IgG1) or ovalbumin plus CpG-DNA (IgG2a).

Isolation and flow cytometry–based definition of splenic dendritic cells. A total of 5×10^6 CD45.1$^+$ Hoxb8-FL cells or unfractionated BM cells were transferred via tail-vein injection into lethally irradiated CD45.2$^+$ recipient mice along with 2×10^5 CD45.2$^+$ BM cells. Seven days after transfer, spleens were removed, cut into small pieces using scissors to obtain a homogenous cell paste, resuspended in spleen dissociation medium (Stem Cell Technologies) and incubated for 30 min at room temperature, followed by incubation for another 5 min in the presence of EDTA (10 mM). Cells were passed through a 40-µm mesh filter and purified by MACS using the Pan-DC isolation kit containing CD11c- and PDCA1-specific antibodies according to the manufacturer's instructions (Miltenyi). Cells were defined based on the following marker combination: pDC, CD11c$^+$PDCA1$^+$; CD8$^+$ cDC, CD11c$^+$PDCA1$^-$CD8α^+CD172a^{low}CD24^{high}; CD8$^-$ cDC, CD11c$^+$PDCA1$^-$CD8α^-CD172a$^+$CD24^{low}.

Evaluation of myeloid and lymphoid potential in bulk cultures *in vitro*. BM– and Hoxb8-FL–derived DCs and macrophages were generated by cultivating unfractionated BM cells or Hoxb8-FL cells for 6 d in standard growth medium (RPMI 1640 (Invitrogen) for DCs or DMEM (Invitrogen) for macrophages, supplemented with 10% (v/v) FCS (Hyclone), 50 mM 2-mercaptoethanol and antibiotics (penicillin G (100 IU/ml) and streptomycin sulfate (100 IU/ml); Invitrogen) containing 5% Flt3L or 2% GM-CSF (DCs), or 30% L-cell–conditioned medium (macrophages) derived from growth factor–producing cell lines. The 5% Flt3L and 2% GM-CSF corresponds to the bioactivity of 70 ng/ml and 7 ng/ml of recombinant growth factors, respectively (Flt3L, R&D; GM-CSF, Becton Dickinson).

In Flt3L and GM-CSF–driven cultures, nonadherent cells were used for subsequent experiments. In cell cultures conditioned with L-cell supernatant, adherent cells were detached by trypsin treatment and used for subsequent experiments. For *in vitro*

differentiation of lymphocyte progenitors, 2×10^5 Hoxb8-FL cells or LSK cells were cocultured on OP9 cells or OP9-DL1 cells that were maintained in alpha-minimum essential medium (Invitrogen) supplemented with 10% FCS (Hyclone), penicillin, streptomycin and recombinant mouse IL-7 (Peprotech, 3 ng/ml) and Flt3L (R&D Systems, 5 ng/ml)[16,37]. Cells were enumerated, filtered through 100-µm cell strainers (BD Falcon) and passaged onto fresh OP9 cells every 3–4 d. LSK cells were isolated from BM by sequential depletion of lineage positive cells by magnetically activated cell sorting (MACS, Miltenyi, lineage cell depletion kit), followed by fluorescence-activated cell sorting based on antibodies against SCA-1 (D7, eBiosciences, dilution 1:100) and c-Kit (2B8, BD Biosciences, dilution 1:100).

Evaluation of myeloid and lymphoid potential in clonal and limiting dilution assays *in vitro*. Myeloid potential of Hoxb8-FL cells and LMPP cells was assessed by clonal assays, seeding one cell per well in 96-well flat-bottom plates by fluorescence-activated cell sorting (FACS) into 100 µl RP-10 with Flt3L-containing supernatant (SN) (5% Flt3L-SN) and L-cell–conditioned supernatant (30%). Formation of typical adherent, myeloid colonies was assessed by light microscopy on day 10 after seeding.

To determine B-cell and T-cell potential, irradiated (15 Gy) OP9 and OP9-DL1 cells were seeded in 50 µl Optimem-10 (Optimem (Invitrogen), supplemented as described for RP-10) into 96-well flat-bottomed plates (1.5×10^4 cells per well). After overnight culture, 50 µl Optimem-10 containing Flt3L, SCF and IL-7 was added to final concentrations of Flt3L-SN (1:50, equivalent to 30 ng/ml recombinant Flt3L), SCF supernatant (1:100, equivalent to 250 ng/ml recombinant SCF) and IL-7 (20 ng/ml). 30, 5 or 1 cell per well of Hoxb8-FL cells or LMPP cells were seeded by FACS. 100 µl of fresh Optimem-10 containing Flt3L (1:50) and IL-7 (10 ng/ml) was added 6 d later and also 13 d later (after removing 100 µl). Colony formation was evaluated by microscopy after 14–16 d (B cells) and 17–20 d (T cells), and Thy1$^-$CD19$^+$CD11b$^-$CD25$^-$CD44$^+$ and Thy1$^+$CD19$^-$CD11b$^-$CD25$^+$CD44$^+$ cells were identified by flow cytometry as B-cell and T-cell progenitors, respectively. Lineage potential was calculated based on extreme limiting dilution analysis (ELDA; http://bioinf.wehi.edu.au/software/elda/)[38].

Evaluation of *in vitro* megakaryocyte potential. Hoxb8-FL cells and LSK cells were seeded in mini-tray plates (Nunc) at a concentration of 1 or 5 cells per well (120 wells each) in 20 µl *X-vivo* 15 medium (Lonza) supplemented with FCS (10% v/v, Hyclone), bovine serum albumin (0.5%, Stemcell Technologies), SCF (50 ng/ml), Flt3L (50 ng/ml), TPO (50 ng/ml), erythropoietin (5 U/ml) and IL-3 (20 ng/ml). Wells were scored for cell growth at different time points up to 8 d. Mk-containing colonies were identified by light microscopy and confirmed morphologically after transferring individual colonies to slides in a cytospin centrifuge and subsequent May-Grünwald–Giemsa staining.

Evaluation of macrophage and erythroid potential *in vitro*. Colony forming cell assays were performed using methylcellulose containing IMDM medium (Methocult, Stemcell Technologies) supplemented with 15% FCS (v/v), 1% bovine serum albumin, recombinant human insulin (10 ng/ml), human transferrin (iron saturated, 200 mg/ml) and various growth factors. To evaluate

CFU-E formation, 2×10^2 Hoxb8-FL cells or 2×10^4 unfractionated BM cells were seeded into 35-mm wells containing methylcellulose medium as described above, which was also supplemented with recombinant human erythropoietin (3 U/ml). Wells were analyzed microscopically for colony formation at different time points up to 10 d. BM-derived colonies were scored after 2 d. To evaluate BFU-E and CFU-M formation, 2×10^2 Hoxb8-FL cells or 2×10^2 LSK cells were seeded into 35-mm wells containing methylcellulose medium as described above, which was also supplemented with recombinant human erythropoietin (3 U/ml), recombinant mouse IL-6 (10 ng/ml), recombinant mouse IL-3 (10 ng/ml) and recombinant mouse SCF (50 ng/ml). Wells were analyzed by microscopy for colony formation at different time points and scored at day 14.

Fluorescence-activated cell sorting. Single-cell suspensions of the spleen were prepared by straining tissues through a 100-µm cell strainer (Becton Dickinson). Peripheral blood was obtained by retro-orbital bleeding. To lyse red blood cells, 100 µl blood were treated with 1.2 ml ammonium chloride solution (Stemcell Technologies) for 10 min on ice, followed by dilution with 10 volumes of PBS containing FBS and centrifugation for 5 min at 450g. Cells obtained from spleens or peripheral blood were blocked with antibodies against CD16/CD32 (eBioscience), followed by staining for cell-surface markers. For intracellular staining, DCs that were first stained for B220 were fixed with 2% formaldehyde in PBS (20 min at 25 °C), followed by incubation with FITC-labeled antibodies against IFNα (or isotype control) and PE-labeled IL-12p40 in PBS containing 0.5% saponin. Flow cytometry analysis was done using a FACSCalibur or FACSCanto II instrument (Becton Dickinson). Single-cell sorting was done using a FACSAria instrument (Becton Dickinson).

Dendritic cell–induced proliferation of T cells *in vitro*. DCs were generated as described in figure legends and incubated with 400 µg/ml chicken ovalbumin (Sigma-Aldrich) for 4 h, washed twice and co-incubated in round-bottom 96-well plates at different concentrations with naive (CD62L^{hi}CD44$^-$CD25$^-$) CD4$^+$ and CD8$^+$ T cells isolated by FACS from spleens of OTI and OTII transgenic mice. In some cases, T cells were labeled with CFSE according to the manufacturer's instructions (Invitrogen). After co-incubation of DCs and T cells for 3 d, T-cell proliferation was either directly determined by flow cytometry (for CFSE-labeled cells) or after an 8-h thymidine pulse in a scintillation beta-counter.

Dendritic cell vaccination and melanoma mouse model. The cDNA encoding a cytoplasmic form of chicken ovalbumin (ovalbumin with deletion of amino acids 19–144; provided by W. Goebel and D. Loeffler, University of Würzburg)[39] was cloned into the MMLV-based retroviral expression vector pQCXIP (BD Clontech), and B16F1 melanoma cells were transduced with replication-deficient, amphotropic retrovirus virus obtained from transiently transfected HEK293T cells. B16F1 cells stably expressing ovalbumin (B16-OVA) were selected using puromycin (10 µg/ml). Hoxb8-FL cells and BM cells were differentiated in the presence of GM-CSF for 9 d, pulsed with ovalbumin (400 µg/ml) for 4 h, washed twice with PBS and stimulated with CpG-DNA for 18 h. Six-week-old C57BL/6 mice were injected subcutaneously with 5×10^5 DCs in 100 µl PBS in the right flank, which had been treated by Nair crème to remove hair. One week later, 2×10^5 B16-OVA cells were injected intradermally in 50 µl PBS in the same area of the right flank, and tumor growth was monitored during time. Mice were sacrificed when the tumors size reached 1 cm^3.

Microarray and principal component analysis (PCA) of hematopoietic cells. Total cellular RNA of four independent Hoxb8-FL cell lines and two BM-derived macrophage populations (BMM) was prepared using TRIzol (Invitrogen), purified using the RNeasy Mini kit (Qiagen), processed and subjected to Affymetrix expression analysis based on MOE v430 chips according to the manufacturer's instructions. Affymetrix MOE v430 CEL file data from Hoxb8-FL cells are available from NCBI GEO (GSE45759). Affymetrix MOE430v2 CEL file data were downloaded from three GEO sources (GSE14833 (progenitors), GSE10246 and GSE6506 (granulocytes)). RMA summarization was performed on all data using Partek Genomics Suite 6.6. To minimize confounding effects of cell culture and source, an ANOVA was applied to the probe sets of progenitor cells to extract genes that best defined cell types based on a published matrix[40]. Probe sets (8,690) that passed the Bonferroni correction at the 0.01 level were retained and used along with the same probe sets from the Hoxb8-FL cells, BMM and granulocytes for visualization by principal component analysis (PCA; Partek Genomic Suite 6.6.). Gene arrays for hematopoietic progenitor cells were generated based on sorted populations using the following markers (provided by S. Zandi and M. Sigvardsson (Linköping University), and D. Bryder (Lund University)): long-term hematopoietic stem cells (Lin$^-$ Sca1$^+$ Kit$^+$ CD34$^-$ flt3$^-$), short-term hematopoietic stem (Lin$^-$ Sca1$^+$ Kit$^+$ CD34$^+$ flt3$^-$), LMPP (Lin$^-$ Sca1$^+$ Kit$^+$ CD34$^+$ flt3$^+$), early thymic progenitor (Lin$^-$ Sca1$^+$ Kit$^+$ CD34$^+$ flt3$^+$ IL7R$^-$), proB (Lin$^-$ CD19$^-$ B220$^+$ CD43$^+$ IgM$^-$), preB (Lin$^-$ CD19$^+$ B220$^+$ CD43$^-$ IgM$^-$), CD4T (Ter119$^-$ Gr1$^-$ Mac1$^-$ Nk1.1$^-$ CD8$^-$ CD4$^+$), PreGM (Lin$^-$ Sca1$^-$ Kit$^+$ CD41$^{-/low}$ CD16/32^{low} CD150$^-$ CD34$^+$ CD9^{low}), granulocyte-macrophage progenitor (GMP) (Lin$^-$ Sca1$^-$ Kit$^+$ CD41$^-$ CD16/32^{high} CD150$^-$ CD34$^+$), MkP (Lin$^-$ Sca1$^-$ Kit$^+$ CD150$^+$ CD41$^+$ CD34$^-$), megakaryocytes and erythroid cells (MkE) (Lin$^-$ Sca1$^-$ Kit$^+$ CD150$^+$ CD41$^+$ CD150$^+$ Endoglin$^-$), preCFUE (Lin$^-$ Sca1$^-$ Kit$^+$ CD150$^+$ CD41$^-$ CD150$^+$ Endoglin$^+$), CFUE (Lin$^-$ Sca1$^-$ Kit$^+$ CD150$^+$ CD41$^-$ CD150$^-$ Endoglin$^+$ Ter119$^-$), ProE (Lin$^-$ Sca1$^-$ Kit$^+$ CD150$^+$ CD41$^-$ CD150$^-$ Endoglin$^+$ Ter119$^+$).

Generation, reconstitution and differentiation of ABIN1-deficient Hoxb8-FL cells. Hoxb8-FL cells from BM of 4-week-old ABIN1-deficient mice were established as described above. Three weeks after infection with the MSCV–ERHBD–Hoxb8 vector, cells were transduced with MSCV-Puro–based (BD Clontech) retroviral vectors expressing wild-type ABIN1 or an ubiquitin-binding deficient mutant of ABIN1, ABN1(Q477E,Q478E), both containing triple Flag and One-STrEP epitope tags (FS) in tandem orientation allowing tandem affinity purification. Two days after infection with virus, transduced cells were selected using puromycin (10 µg/ml) and continuously maintained in culture for another 14 d. For subsequent differentiation, 3×10^7 cells were washed twice with PBS containing FCS and resuspended at a concentration of 1×10^5 cells/ml in GM-CSF–conditioned RP-10 as described for generation of GM-CSF-derived DCs. Cells were fed with GM-CSF–containing medium after 3 d and 5 d. After 8 d, 8×10^8 cells were collected by centrifugation and snap freezing using methanol on dry ice.

Tandem affinity purification. Frozen cell pellets were dissolved in lysis buffer ((LB) 20 mM HEPES-KOH (pH 7.5), 150 mM NaCl, 1.5 mM MgCl, 1 mM EDTA, 1 mM PMSF, 10% glycerol, 1 mM orthovanadate, 10 mM β-glycerophosphate, 5 mM 4-nitrophenyl-phosphate, 10 mM sodium fluoride and 'complete protease inhibitors' (Roche)) containing 0.5% NP40 for 20 min. Samples were cleared by centrifugation (10 min, 1,500*g*, 4 °C), and incubated with Strep-Tactin Superflow beads (IBA) for 90 min. Beads were collected by centrifugation, washed and proteins were eluted in 1 ml of LB containing desthiobiotin (5 mM; Sigma-Aldrich) and 0.1% NP40. Proteins were recaptured on columns containing M2 Flag beads (Sigma-Aldrich), washed and eluted at low pH (0.1 mM glycine (pH 3.5) followed by TCA precipitation, separation on a 4–12% Bis-Tris gel (Bio-Rad) and staining with SYPRO Ruby (Invitrogen).

Sample preparation for mass spectrometry analysis. Individual gel lanes containing the immunopurified samples were excised into 15 bands, each of which was cut into small plugs, washed with 50% (v/v) acetonitrile and destained by repeated incubations in 100 mM ammonium bicarbonate (pH 8.0) containing 50% acetonitrile. Gel plugs were reduced (10 mM DTT, 1 h at 37 °C), alkylated (50 mM iodoacetamide, 45 min at room temperature in the dark), washed twice with 50% acetonitrile in 50 mM ammonium bicarbonate, dried in a SpeedVac (Savant) and rehydrated for 10 min in 10 µl of 0.2 µg/µl trypsin. Then 25 µl of ammonium bicarbonate (25 mM, pH 8.0) was added and incubated for 12 h at 37 °C, followed by peptide extraction using 5–10 µl of 0.2% formic acid. The peptide-containing solution was transferred to a sample vial for liquid chromatography–tandem mass spectrometry (LC-MS/MS) analysis.

Electrospray ionization Orbitrap mass spectrometry analysis. LC-MS/MS analysis was performed using a Thermo Fisher LTQ Orbitrap XL mass spectrometer in line with a nanoAcquity ultra-performance LC system (Waters Corporation). Tryptic peptides were loaded onto a 'precolumn' (Symmetry C18, 180 µm in diameter × 20 mm, 5-µm particle) (Waters Corporation) which was connected through a zero dead-volume union to the analytical column (BEH C18, 75 µm in diameter × 100 mm, 1.7-µm particle; Waters Corporation). The peptides were eluted over a gradient (0−70% B in 60 min, 70−100% B in 10 min, where B = 70% (v/v) acetonitrile and 0.2% formic acid) at a flow rate of 250 nl/min and were introduced online into the Orbitrap mass spectrometer using electrospray ionization. Data-dependent scanning was incorporated to select the 10 most abundant ions (one microscan per spectrum; precursor isolation width 2.0 Da; 35% collision energy; 30-ms ion activation; 30 s exclusion duration; 15 s repeat duration; repeat count of 2) from a full-scan mass spectrum for fragmentation by collision-activated dissociation.

Database search. Product ions (*b/y*-type ions) were queried in an automated database search against a protein database (Swissprot 2012_10 (538259 sequences; 191113170 residues, *Mus musculus* subset)) by the Mascot search algorithm. The following residue modifications were allowed in the search: carbamidomethylation on cysteine (fixed modification) and oxidation on methionine (variable modification). Mascot was searched with a precursor ion tolerance of 100 p.p.m. and a fragment ion tolerance of 0.7 Da and using the automatic decoy database-searching tool in Mascot. The identifications from the automated search were verified by manual inspection of the raw data.

Microscopy. Images were obtained using the microscopes Axio Scope.A1 and Axiovert 40 CFL (Zeiss) for cells stained with May-Grünwald and Giemsa and live cells, respectively. Software used was Axiovision 4 (Zeiss).

35. Stuehr, D.J. & Nathan, C.F. Nitric oxide. A macrophage product responsible for cytostasis and respiratory inhibition in tumor target cells. *J. Exp. Med.* **169**, 1543–1555 (1989).
36. Tora, L. *et al.* The cloned human oestrogen receptor contains a mutation which alters its hormone binding properties. *EMBO J.* **8**, 1981–1986 (1989).
37. Schmitt, T.M. & Zuniga-Pflucker, J.C. T-cell development, doing it in a dish. *Immunol. Rev.* **209**, 95–102 (2006).
38. Hu, Y. & Smyth, G.K. ELDA: extreme limiting dilution analysis for comparing depleted and enriched populations in stem cell and other assays. *J. Immunol. Methods* **347**, 70–78 (2009).
39. Loeffler, D.I., Schoen, C.U., Goebel, W. & Pilgrim, S. Comparison of different live vaccine strategies *in vivo* for delivery of protein antigen or antigen-encoding DNA and mRNA by virulence-attenuated *Listeria monocytogenes*. *Infect. Immun.* **74**, 3946–3957 (2006).
40. Di Tullio, A. *et al.* CCAAT/enhancer binding protein alpha (C/EBP(alpha))-induced transdifferentiation of pre-B cells into macrophages involves no overt retrodifferentiation. *Proc. Natl. Acad. Sci. USA* **108**, 17016–17021 (2011).